On-Surface Synthesis of Single-Layered Two-Dimensional Covalent Organic Frameworks via Solid−Vapor Interface Reactions

Xuan-He Liu,[†,‡] Cui-Zhong Guan,[†,‡] San-Yuan Ding,[§] Wei Wang,[§] Hui-Juan Yan,[†] Dong Wang,*[,†] and Li-Jun Wan*[,†]

[†]Key Laboratory of Molecular Nanostructure and Nanotechnology and Beijing National Laboratory for Molecular Sciences, Institute of Chemistry, Chinese Academy of Sciences (CAS), Beijing 100190, P. R. China

[‡]University of CAS, Beijing 100049, P. R. China

[§]State Key Laboratory of Applied Organic Chemistry, Lanzhou University, Lanzhou, Gansu 730000, P. R. China

S *Supporting Information*

ABSTRACT: Surface covalent organic frameworks (SCOFs), featured by atomic thick sheet with covalently bonded organic building units, are promised to possess unique properties associated with reduced dimensionality, well-defined in-plane structure, and tunable functionality. Although a great deal of effort has been made to obtain SCOFs with different linkages and building blocks via both "top-down" exfoliation and "bottom-up" surface synthesis approaches, the obtained SCOFs generally suffer a low crystallinity, which impedes the understanding of intrinsic properties of the materials. Herein, we demonstrate a self-limiting solid−vapor interface reaction strategy to fabricate highly ordered SCOFs. The coupling reaction is tailored to

take place at the solid−vapor interface by introducing one precursor via vaporization to the surface preloaded with the other precursor. Following this strategy, highly ordered honeycomb SCOFs with imine linkage are obtained. The controlled formation of SCOFs in our study shows the possibility of a rational design and synthesis of SCOFs with desired functionality.
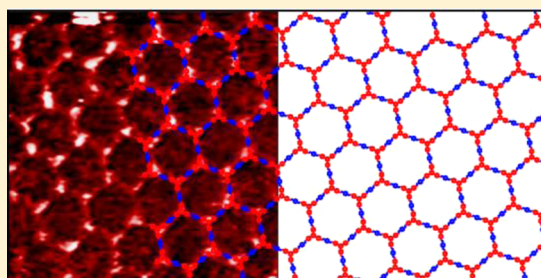
1. INTRODUCTION

Covalent organic frameworks (COFs), featured by the crystalline extended organic structures with covalently bonded building blocks, have attracted great attention since the first COF was reported in 2005.[1] Aside from gas storage[1−3] and catalytic application,[4] interesting electronic and optoelectronic properties[5−14] of the bulk COF materials have been demonstrated by engineering different functional building blocks into COF backbones.[13]

Surface covalent organic networks (SCOFs) are analogues to bulk COF materials except that they are ideally one-atom thick. The exotic electronic properties demonstrated on 2D inorganic materials, such as graphene and metal chalcogenide,[15,16] reveal the importance of dimensionality and well-defined in-plane crystallinity for the materials properties. The SCOFs, especially those with backbones containing extended π conjugation, may also exhibit interesting in-plane carrier transportation behavior and are promising materials for applications in molecular electronics, sensors, and optoelectronic devices.[17] Theoretical calculations predict that electronic properties of the SCOFs can be controlled by tailoring the topology of networks and the chemical properties of the building blocks as well.[18−20] Generally, the approaches to obtain SCOFs on solid supports can be classified into the "top-down" and "bottom-up" strategies.[21−23] Although the "top-down" exfoliation of layered bulk crystals is effective to obtain single-layered graphene and

other metal chalcogenide materials,[16] its application to bulk crystalline COF materials turns out to be practically difficult due to the unavailability of large-sized COF crystals and the tendency of multilayer formation after exfoliations.[24−26] On the other hand, on-surface "bottom-up" synthesis is considered to be promising to construct SCOFs. Different types of organic coupling reactions, such as Ulmann radical coupling, polyimide formation, imine coupling, boronic anhydridation reaction, etc., have been accomplished directly on surfaces.[27−43] Unfortunately, the prepared 2D SCOFs usually suffer from small domain sizes and large amounts of topological defects.

The special features of covalently bonded linkages require novel synthesis strategies for high-quality SCOFs. The formation of fully developed 2D SCOFs, in contrast to the 1D linear polymers, requires a precise control over the conformation of each building units. This turns out to be especially challenging considering the high bond strength and poor reversibility associated with the covalent bond. Recently, a strategy through the thermodynamic equilibrium manipulation has been developed to construct highly ordered 2D boroxine-based covalent networks.[44,45] However, the synthesis of SCOFs with high quality based on bicomponent coupling reactions still faces a great challenge.

2. RESULTS

Herein, we propose a self-limiting solid—vapor interface reaction method to grow large-scale highly ordered bicomponent 2D SCOFs. Figure 1 shows the scheme for the
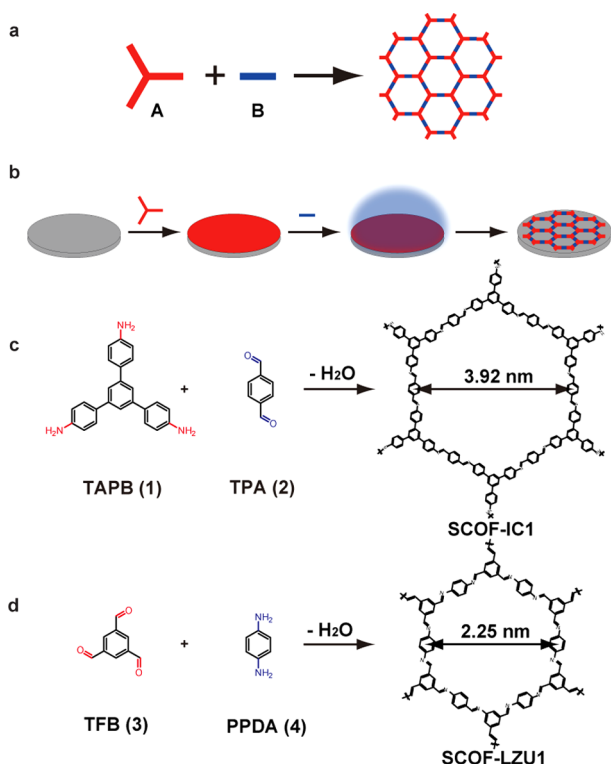

Figure 1. Schematic diagram of SCOFs formation. (a) Condensation of two precursors A and B carrying different reactive partner groups results in the formation of SCOF. (b) Scheme diagram for solid—vapor interface reaction. (c, d) Condensation of trigonal precursors TAPB or TFB and linear precursors TPA or PPDA can form SCOF-IC1 or SCOF-LZU1, respectively. The expected lattice parameters are indicated.

experimental design. Two different molecules with suitable reactive partner groups are selected as reaction precursors to form a 2D network. As shown in Figure 1b, one precursor (A) is first preloaded onto the substrate through drop-casting. Precursor B is then introduced, and the whole system is thereafter sealed up in a closed reactor with the presence of $CuSO_4 \cdot 5H_2O$ as thermodynamic regulation agent.[44] By heating the reactor to a designated temperature, precursor B will vaporize and then land on the surface covered with precursor A. Accordingly, the covalent bond can form at the solid—vapor interface, leading to the growth of high quality SCOFs. During this process, the growth is determined by the gas phase dosing of precursor B, and the unwanted formation of disordered oligomers is effectively minimized. In our study, an imine bond has been chosen as the linkage for the SCOFs due to many merits of imine formation reaction, such as the easily accessible building blocks, high reversibility, and mild reaction conditions. The imine bond is widely known as a dynamic covalent bond and has been applied successfully to prepare crystalline bulk COF materials and organic cages recently.[4,46−48] By employing the self-limiting solid—vapor interface reaction method, the synthesis of high-quality SCOFs with low defect density and large domain size is successfully achieved. The reaction

equations for synthesis of SCOF-IC1 and SCOF-LZU1 are shown in Figure 1c,d, respectively.

2.1. Synthesis of SCOFs. Figure 2a shows a representative STM image of SCOF-IC1 obtained by condensation of 1,3,5-
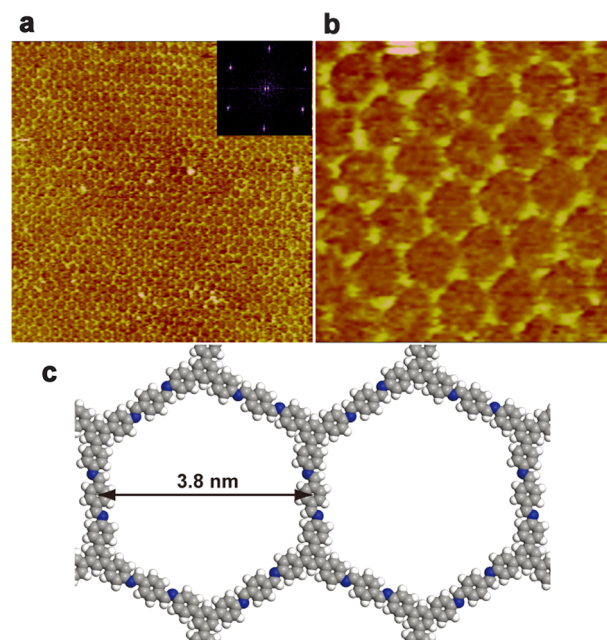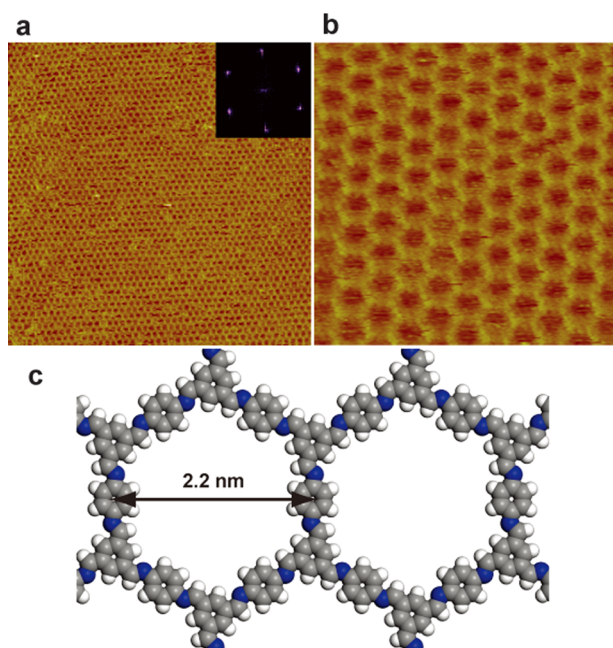

Figure 2. STM images and a structural model for SCOF-IC1. (a) Large-scale STM image (100×100 nm^2) of SCOF-IC1 with the inset depicting the corresponding FFT spectrum of the STM image. (b) High resolution STM image (20×20 nm^2) of SCOF-IC1. (c) A structural model with the measured structural parameter for SCOF-IC1. Imaging conditions: (a) V_{bias} = 700 mV, I_t = 500 pA; (b) V_{bias} = 693 mV, I_t = 450 pA.

tris(4-aminophenyl)benzene (TAPB, 1) on highly oriented pyrolytic graphite (HOPG) and gaseous terephthaldicarbox-aldehyde (TPA, 2) in a closed system after heating at 150 °C for 3 h. A highly ordered honeycomb network structure is disclosed. The two-dimensional fast Fourier transform (FFT) of image in the inset shows well-defined 6-fold symmetry. The typical domain size of two-dimensional SCOF-IC1 can reach more than 200×200 nm^2 with few defects (see Supporting Information). By comparing with the atomic image of underlying HOPG lattice, the SCOF-IC1 networks are determined to grow at fixed orientation relative to the HOPG surface (see Supporting Information). Figure 2b displays a high-resolution STM image of SCOF-IC1. The lattice parameter of the structure is measured to be 3.8 ± 0.2 nm, which agrees well with the expected size of 3.92 nm by density functional theory (DFT) calculation, and thus confirms the covalent formation of the imine-linked SCOF-IC1.

Similarly, we can obtain SCOF-LZU1 by condensation of precursors equipped with 3 aldehyde groups and 2 amino groups, namely, 1,3,5-triformyl-benzene (TFB, 3) and p-phenylenediamine (PPDA, 4). Figure 3a reveals a highly ordered honeycomb network of SCOF-LZU1. The two-dimensional FFT of image in the inset shows well-defined 6-fold symmetry. The typical domain size of two-dimensional SCOF-LZU1 with rare defects can attain more than 350×350 nm^2 (see Supporting Information). Figure 3b displays a high-resolution STM image of SCOF-LZU1. Structural analysis of the network shows the lattice parameter 2.2 ± 0.2 nm is in

Figure 3. STM images and a structural model for SCOF-LZU1. (a) Large-scale STM image (100×100 nm^2) of SCOF-LZU1 with the inset depicting the corresponding FFT spectrum of the STM image. (b) High resolution STM image (20×20 nm^2) of SCOF-LZU1. (c) A structural model with the measured structural parameter for SCOF-LZU1. Imaging conditions: $V_{bias} = 620$ mV, $I_t = 536$ pA.

excellent agreement with the 2.25 nm size predicted by DFT calculation. X-ray photoelectron spectroscopy (XPS) analysis provides additional evidence for the formation of imine bond. The C 1s spectrum can be deconvoluted as a band at 284.4 eV, corresponding to the C in SCOF backbone and HOPG and a band at 285.1 eV, attributed to the C in imine bond. At the same time, the N 1s spectrum can be deconvoluted as two bands at 398.6 and 399.7 eV, which are assigned to the N in imine bonding structure and N in the unreacted amine group in PPDA, respectively.[49] The frames of SCOFs show nearly uniform contrast in high resolution STM image, further supporting the formation of the fully conjugated, covalent bond-linked network, as expected. SCOF-LZU1 can remain on HOPG without obvious decomposition after being stored in an ambient environment for more than 18 days (see Supporting Information). The combined features of SCOFs, including stability, orderliness, and completely π-conjugated architecture promise their potential applications in optoelectronic devices.

2.2. Effect of Precursor Coverage. We find that the coverage of precursors on HOPG, temperature, and the reaction equilibrium agent (H_2O releasing compounds) are the important factors affecting the quality of SCOFs. Taking SCOF-IC1 as an example, Supporting Information Figure S5 shows a series of STM images of SCOF-IC1 obtained with HOPG loaded with different coverage of TAPB (1). When 5 μL of $\sim 10^{-5}$ M tetrahydrofuran (THF) solution is used to cast TAPB film, scattered SCOF-IC1 flakes are obtained. The SCOF-IC1 flakes are always arranged with the same orientation, which implies the orientated growth of the SCOF-IC1 network on HOPG substrate (Supporting Information Figures S2 and S6). The high-quality SCOF with typical domain size of more than 200×200 nm^2 can be routinely obtained (see Supporting Information). When a TAPB (1) solution with concentration of $\sim 10^{-4}$ M is used to

cast thin film, the domain size starts shrinking, and the domain boundaries are formed by coalescing neighboring domains together with zigzag borderlines (see Supporting Information). We thus speculate that, after the nuclei formation, the SCOF-IC1 grows until neighboring domains meet together to form domain boundaries. The domains possess the same orientation as determined by their nuclei on the HOPG surface. The domain size is affected by the number of nuclei and thereby the coverage of TAPB (1). Interestingly, we notice that the domain boundary is always terminated by the triangular shape TAPB (1) molecules (see Supporting Information), which implies the excess of TAPB (1) relative to the vaporized precursor TPA (2) on the HOPG surface. Finally, deteriorative results of disordered clusters emerge, when TAPB (1) coverage is even higher.

2.3. Effect of Temperature. The reaction temperature also has a profound effect on SCOF-IC1 formation. Figure 4 shows
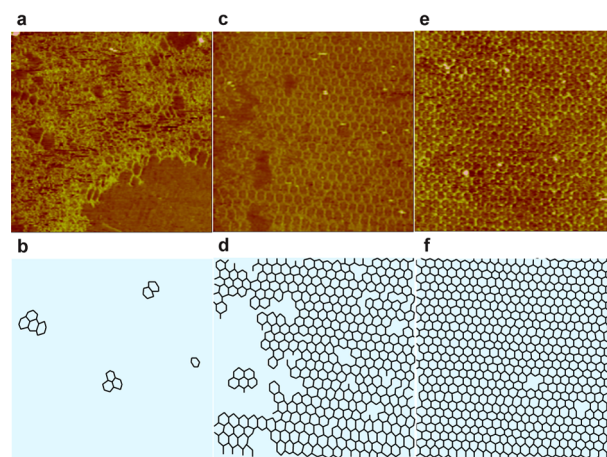
Figure 4. Effect of reaction temperature on SCOF-IC1 growth. STM images (a, c, e, 80×80 nm^2) and the corresponding delineated images (b, d, f) of SCOF-IC1 obtained at 110 °C (a, b), 120 °C (c, d), and 150 °C (e, f). The quality of SCOF is qualitatively evaluated by counting the coverage of hexagon on surface. Imaging conditions: (a) $V_{bias} = 762$ mV, $I_t = 500$ pA; (b) $V_{bias} = 700$ mV, $I_t = 500$ pA; (c) $V_{bias} = 700$ mV, $I_t = 500$ pA.

representative STM images of SCOF-IC1 obtained at different reaction temperatures. At 110 °C, many oligomers tend to emerge, and only a few networks are formed. The results are ascribed to an insufficient vapor pressure of TAP at lower temperatures or low diffusion rate of precursor TAPB (1) on HOPG surface. The disordered oligomers act on defects and are detrimental for large-scale network formation. Statistical analysis indicates that only 2% of the surface is covered by the six-membered rings of the covalent network in SCOF-IC1 flakes (Figure 4a,b). With the elevation of temperature to 120 °C, the SCOF-IC1 networks can undergo orientated growth after nuclei formation. Nevertheless, a few topological defects always exist in the SCOF-IC1 flakes with order degree of 63% (Figure 4c,d). At 150 °C, large-scale SCOF-IC1 networks with few topological defects can be obtained, and the coverage of six-member rings can attain to 98% (Figure 4e,f). The evaporation rate of precursor TPF (2) and the diffusion rate of TAPB (1) on surface are believed to be optimal to ensure the effective attachment of TPF (2) and TAPB (1) in SCOF-IC1 flakes successively. At the same time, the reversibility of the reaction can be elevated by increasing the reaction temperature

following the principle of Le Chatelier. Therefore, the ability of self-healing can be boosted at higher reaction temperature leading to the high-quality SCOF. However, at even higher reaction temperature 180 °C, only bare small networks can be observed on HOPG surfaces by STM, possibly due to the sublimation of precursors, the decomposition of SCOF-IC1 networks, and/or uncontrollable complex side reactions between precursors (see Supporting Information).

2.4. Effect of Thermodynamic Regulation Agent.

The designated amount of H_2O releasing agent, typically $CuSO_4 \cdot 5H_2O$, is always placed in the closed autoclaves during the SCOFs synthesis process. The H_2O releasing agent can release water vapor during the heating process and increase the reversibility of aldehyde–amine coupling reaction. The regulation of the thermodynamic equilibrium for the covalent bond formation by introducing a small amount of water into a closed reaction system has been previously demonstrated for the synthesis of SCOF via boronic anhydridation.[44] Therefore, the same principle is operated in the present system, and the details are not described here.

3. DISCUSSION

Figure 5a shows the schematic growth process of SCOFs. When the vapor pressure of precursor B builds up during
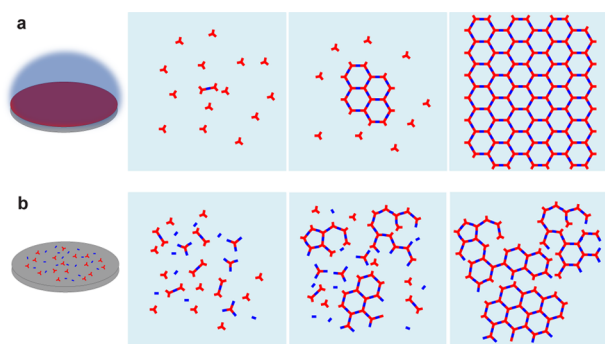
Figure 5. Schematic diagrams of the proposed formation mechanism of the SCOF. (a) The nucleation and enlargement of the SCOF flakes by self-limiting solid–vapor interface reaction strategy. (b) The less-ordered SCOF formation process in the control experiments by heating the substrate preloaded with two precursors.

heating the reactor, the coupling of reactive groups separately carried by precursors A and B results in the nucleation of the SCOF. Since the rate at which precursor B reaches the surface and reacts is very low, the freshly vaporized precursor B, or the freshed formed small oligomer, can diffuse on the surface and attach to the available SCOF nuclei, resulting in the growth of the SCOF. In this way, the unwanted growth of the thermodynamically unstable oligomers and the SCOF defects are minimized. In addition, the SCOF is always terminated by the reactive groups carried by precursor A, due to the quick diffusion and excess of precursor A available relative to the vaporized precursor B on HOPG surface. The feature of the present method is that the reaction takes place on the vapor–solid interface and is self-limited by capping reactive groups of precursor A. Following this method, highly ordered 2D networks with large domain size and completely π-conjugated architectures are obtained. The time-dependent SCOF-LZU1 flake growth process from HOPG edge to cover the whole terrace (see Supporting Information) provides supportive evidence for the mechanism proposed above. The order of

monomer introduction is determined by the vapor pressure of the precursors. No expected SCOFs are formed if the order of monomer introduction is reversed, since higher vapor pressure precursor B would have been fully vaporized before precursor A reaches the surfaces (see Supporting Information).

We also carried out the control experiments to construct SCOFs by heating the HOPG surfaces loaded with the two starting molecules together with water in a closed system, as schematically shown in Figure 5b. The molecular-level mixing of precursors on surfaces results in the immediate occurrence of large amounts of nuclei. The resulting oligomers do not have enough mobility and flexibility to reach the most stable conformations thermodynamically, thus resulting in the formation of the SCOF with small ordered domains and lots of irregular polygons (see Supporting Information). The scenarios can be pretty deteriorative when high-molecular-weight and thus low-mobility precursors are employed, as exemplified in Supporting Information.

4. CONCLUSION

In summary, we demonstrate a self-limiting solid–vapor interface reaction strategy for the construction of large-scale high-quality SCOFs. This strategy can be a general protocol to accomplish other kinds of bicomponent chemical reactions, not limited to Schiff-base reaction, the specific example we reported here. In contrast to the reactions that happened in solution, stoichiometric ratio control of precursors is not strictly required for the solid–vapor interface reaction. A mechanism of nucleation and orientated growth for the self-limiting solid–vapor interface reaction method is proposed. Further application of protocol developed in the present work to other coupling reactions will pave the way to rational design and synthesis of single-layered SCOFs with desired functionality.

■ ASSOCIATED CONTENT

ⓢ Supporting Information

Experimental methods and supplementary STM figures. This material is available free of charge via the Internet at http://pubs.acs.org.

■ AUTHOR INFORMATION

Corresponding Author
wangd@iccas.ac.cn; wanlijun@iccas.ac.cn
Author Contributions
X.-H.L. and C.-Z.G. contributed equally to this work.
Notes
The authors declare no competing financial interest.

■ ACKNOWLEDGMENTS

■ REFERENCES

(1) Côté, A. P.; Benin, A. I.; Ockwig, N. W.; O'Keeffe, M.; Matzger, A. J.; Yaghi, O. M. *Science* **2005**, *310*, 1166.
(2) Kandambeth, S.; Mallick, A.; Lukose, B.; Heine, T.; Banerjee, R.; Mane, M. *J. Am. Chem. Soc.* **2012**, *134*, 19524.

(3) Tilford, R. W.; Gemmill, W. R.; zur Loye, H.-C.; Lavigne, J. J. *Chem. Mater.* **2006**, *18*, 5296.

(4) Ding, S.-Y.; Gao, J.; Wang, Q.; Zhang, Y.; Song, W.-G.; Su, C.-Y.; Wang, W. *J. Am. Chem. Soc.* **2011**, *133*, 19816.

(5) Wan, S.; Gándara, F.; Asano, A.; Furukawa, H.; Saeki, A.; Dey, S. K.; Liao, L.; Ambrogio, M. W.; Botros, Y. Y.; Duan, X.; Seki, S.; Stoddart, J. F.; Yaghi, O. M. *Chem. Mater.* **2011**, *23*, 4094.

(6) Jin, S.; Ding, X.; Feng, X.; Supur, M.; Furukawa, K.; Takahashi, S.; Addicoat, M.; El-Khouly, M. E.; Nakamura, T.; Irle, S. *Angew. Chem., Int. Ed.* **2013**, *52*, 2017.

(7) Dogru, M.; Handloser, M.; Auras, F.; Kunz, T.; Medina, D.; Hartschuh, A.; Knochel, P.; Bein, T. *Angew. Chem., Int. Ed.* **2013**, *52*, 2920.

(8) Spitler, E. L.; Dichtel, W. R. *Nat. Chem.* **2010**, *2*, 672.

(9) Spitler, E. L.; Koo, B. T.; Novotney, J. L.; Colson, J. W.; Uribe-Romo, F. J.; Gutierrez, G. D.; Clancy, P.; Dichtel, W. R. *J. Am. Chem. Soc.* **2011**, *133*, 19416.

(10) Spitler, E. L.; Colson, J. W.; Uribe-Romo, F. J.; Woll, A. R.; Giovino, M. R.; Saldivar, A.; Dichtel, W. R. *Angew. Chem., Int. Ed.* **2012**, *51*, 2623.

(11) Dogru, M.; Sonnauer, A.; Zimdars, S.; Döblinger, M.; Knochel, P.; Bein, T. *CrystEngComm* **2013**, *15*, 1500.

(12) Ren, S.; Bojdys, M. J.; Dawson, R.; Laybourn, A.; Khimyak, Y. Z.; Adams, D. J.; Cooper, A. I. *Adv. Mater.* **2012**, *24*, 2357.

(13) Feng, X.; Ding, X.; Jiang, D. *Chem. Soc. Rev.* **2012**, *41*, 6010.

(14) Colson, J. W.; Woll, A. R.; Mukherjee, A.; Levendorf, M. P.; Spitler, E. L.; Shields, V. B.; Spencer, M. G.; Park, J.; Dichtel, W. R. *Science* **2011**, *332*, 228.

(15) Bonaccorso, F.; Sun, Z.; Hasan, T.; Ferrari, A. C. *Nat. Photonics* **2010**, *4*, 611.

(16) Mas-Ballesté, R.; Gómez-Navarro, C.; Gómez-Herrero, J.; Zamora, F. *Nanoscale* **2011**, *3*, 20.

(17) Perepichka, D. F.; Rosei, F. *Science* **2009**, *323*, 216.

(18) Abraham, F. K.; Nelson, D. R. *Science* **1990**, *249*, 393.

(19) Baughman, R. H.; Eckardt, H.; Kertez, M. *J. Chem. Phys.* **1987**, *87*, 6687.

(20) Tanaka, K.; Kosai, N.; Maruyama, H.; Kobayashi, H. *Synth. Met.* **1998**, *92*, 253.

(21) Sakamoto, J.; van Heijst, J.; Lukin, O.; Schlüter, A. D. *Angew. Chem., Int. Ed.* **2009**, *48*, 1030.

(22) Elemans, J. A. A. W.; Lei, S.; De Feyter, S. *Angew. Chem., Int. Ed.* **2009**, *48*, 7298.

(23) Barth, J. V.; Costantini, G.; Kern, K. *Nature* **2005**, *437*, 671.

(24) Berlanga, I.; Ruiz-González, M. L.; González-Calbet, J. M.; Fierro, J. L. G.; Mas-Ballesté, R.; Zamora, F. *Small* **2011**, *7*, 1207.

(25) Kissel, P.; Erni, R.; Schweizer, W. B.; Rossell, M. D.; King, B. T.; Bauer, T.; Götzinger, S.; Schlüter, A. D.; Sakamoto, J. *Nat. Chem.* **2012**, *4*, 287.

(26) Li, M.; Schluter, A. D.; Sakamoto, J. *J. Am. Chem. Soc.* **2012**, *134*, 11721.

(27) Grill, L.; Dyer, M.; Lafferentz, L.; Persson, M.; Peters, M. V.; Hecht, S. *Nat. Nanotechnol.* **2007**, *2*, 687.

(28) In't Veld, M.; Iavicoli, P.; Haq, S.; Amabilino, D. B.; Raval, R. *Chem. Commun.* **2008**, 1536.

(29) Treier, M.; Richardson, N. V.; Fasel, R. *J. Am. Chem. Soc.* **2008**, *130*, 14054.

(30) Weigelt, S.; Busse, C.; Bombis, C.; Knudsen, M. M.; Gothelf, K. V.; Lægsgaard, E.; Besenbacher, F.; Linderoth, T. R. *Angew. Chem., Int. Ed.* **2008**, *47*, 4406.

(31) Tanoue, R.; Higuchi, R.; Enoki, N.; Miyasato, Y.; Uemura, S.; Kimizuka, N.; Stieg, A. Z.; Gimzewski, J. K.; Kunitake, M. *ACS Nano* **2011**, *5*, 3923.

(32) Zwaneveld, N. A. A.; Pawlak, R. m.; Abel, M.; Catalin, D.; Gigmes, D.; Bertin, D.; Porte, L. *J. Am. Chem. Soc.* **2008**, *130*, 6678.

(33) Matena, M.; Riehm, T.; Stöhr, M.; Jung, T. A.; Gade, L. H. *Angew. Chem., Int. Ed.* **2008**, *47*, 2414.

(34) Jensen, S.; Früchtl, H.; Baddeley, C. J. *J. Am. Chem. Soc.* **2009**, *131*, 16706.

(35) Marele, A. C.; Mas-Balleste, R.; Terracciano, L.; Rodríguez-Fernández, J.; Berlanga, I.; Alexandre, S.; Otero, R.; Gallego, J. M.; Zamora, F.; Gómez-Rodríguez, J. M. *Chem. Commun.* **2012**, *48*, 6779.

(36) Schmitz, C. H.; Ikonomov, J.; Sokolowski, M. *J. Phys. Chem. C* **2011**, *115*, 7270.

(37) Abel, M.; Clair, S.; Ourdjini, O.; Mossoyan, M.; Porte, L. *J. Am. Chem. Soc.* **2011**, *133*, 1203.

(38) Blunt, M. O.; Russell, J. C.; Champness, N. R.; Beton, P. H. *Chem. Commun.* **2010**, *46*, 7157.

(39) Lipton-Duffin, J. A.; Ivasenko, O.; Perepichka, D. F.; Rosei, F. *Small* **2009**, *5*, 592.

(40) Lipton-Duffin, J.; Miwa, J.; Kondratenko, M.; Cicoira, F.; Sumpter, B.; Meunier, V.; Perepichka, D.; Rosei, F. *Proc. Natl. Acad. Sci. U.S.A.* **2010**, *107*, 11200.

(41) Bieri, M.; Treier, M.; Cai, J.; Aït-Mansour, K.; Ruffieux, P.; Gröning, O.; Gröning, P.; Kastler, M.; Rieger, R.; Feng, X.; Müllen, K.; Fasel, R. *Chem. Commun.* **2009**, *45*, 6919.

(42) Gutzler, R.; Walch, H.; Eder, G.; Kloft, S.; Heckl, W. M.; Lackinger, M. *Chem. Commun.* **2009**, 4456.

(43) Cai, J.; Ruffieux, P.; Jaafar, R.; Bieri, M.; Braun, T.; Blankenburg, S.; Muoth, M.; Seitsonen, A. P.; Saleh, M.; Feng, X. *Nature* **2010**, *466*, 470.

(44) Guan, C. Z.; Wang, D.; Wan, L. J. *Chem. Commun.* **2012**, *48*, 2943.

(45) Dienstmaier, J. F.; Gigler, A. M.; Goetz, A. J.; Knochel, P.; Bein, T.; Lyapin, A.; Reichlmaier, S.; Heckl, W. M.; Lackinger, M. *ACS Nano* **2011**, *5*, 9737.

(46) Uribe-Romo, F. J.; Hunt, J. R.; Furukawa, H.; Klock, C.; O'Keeffe, M.; Yaghi, O. M. *J. Am. Chem. Soc.* **2009**, *131*, 4570.

(47) Jin, Y.; Zhu, Y.; Zhang, W. *CrystEngComm* **2013**, *15*, 1484.

(48) Tozawa, T.; Jones, J. T.; Swamy, S. I.; Jiang, S.; Adams, D. J.; Shakespeare, S.; Clowes, R.; Bradshaw, D.; Hasell, T.; Chong, S. Y. *Nat. Mater.* **2009**, *8*, 973.

(49) Golczak, S.; Kanciurzewska, A.; Fahlman, M.; Langer, K.; Langer, J. J. *Solid State Ionics* **2008**, *179*, 2234−2239.